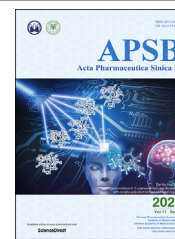




Chinese Pharmaceutical Association
Institute of Materia Medica, Chinese Academy of Medical Sciences

Acta Pharmaceutica Sinica B

www.elsevier.com/locate/apsb
www.sciencedirect.com



ORIGINAL ARTICLE

Tripodalsporormielones A–C, unprecedented cage-like polyketides with complex polydent bridged and fused ring systems



Guodong Chen^{a,†}, Bingxin Zhao^{b,†}, Meijuan Huang^a, Jia Tang^a,
Yanbing Li^{a,c}, Liangdong Guo^d, Rongrong He^{a,c}, Dan Hu^{a,*},
Xinsheng Yao^a, Hao Gao^{a,*}

^aInstitute of Traditional Chinese Medicine & Natural Products, College of Pharmacy/Guangdong Province Key Laboratory of Pharmacodynamic Constituents of TCM and New Drugs Research, Jinan University, Guangzhou 510632, China

^bDepartment of Chemistry, College of Chemistry and Materials Science, Jinan University, Guangzhou 510632, China

^cGuangdong Engineering Research Center of Chinese Medicine & Disease Susceptibility, Jinan University, Guangzhou 510632, China

^dState Key Laboratory of Mycology, Institute of Microbiology, Chinese Academy of Sciences, Beijing 100190, China

Received 17 February 2021; received in revised form 12 April 2021; accepted 2 May 2021

KEY WORDS

Tripodalsporormielones;
Cage-like polyketides;
3-Methylorcinolaldehyde;
Alzheimer's disease

Abstract A chemical investigation on *Sporormiella* sp. led to the isolation and structural elucidation of tripodalsporormielones A–C (1–3), a new class of polyketide possessing unprecedented cage-like skeletons with polydent bridged and fused ring systems. These polyketides with cage-like skeletons were characterized as a high non-protonated carbon-containing system, which resulted in few HMBC correlations observed and made the accurate structures hard to be obtained by NMR. Especially, some signals of non-protonated sp^2 carbons are weak and even unobservable in compound **1**. In order to establish the structure of **1**, the calculated NMR with DP4 evaluation was applied to determine the structure from the plausible structure candidates obtained from the detailed NMR analysis. Based on NMR experiments and calculated NMR, the structures of isolated compounds were established and confirmed by X-ray technology. Through chiral isolation, the optically pure enantiomers of **1** and **3** were obtained, and their absolute configurations were determined based on ECD quantum chemical calculation. Based on the isolated compounds and our previous work, **1–3** would be derived from 3-methylorcinolaldehyde, and their

*Corresponding authors. Tel./fax: +86 20 85228369.

E-mail addresses: thudan@jnu.edu.cn (Dan Hu), tghao@jnu.edu.cn (Hao Gao).

†These authors made equal contributions to this work.

Peer review under responsibility of Chinese Pharmaceutical Association and Institute of Materia Medica, Chinese Academy of Medical Sciences.

<https://doi.org/10.1016/j.apsb.2021.05.001>

2211-3835 © 2021 Chinese Pharmaceutical Association and Institute of Materia Medica, Chinese Academy of Medical Sciences. Production and hosting by Elsevier B.V. This is an open access article under the CC BY-NC-ND license (<http://creativecommons.org/licenses/by-nc-nd/4.0/>).

plausible biosynthetic mechanism was proposed. Furthermore, **1** exhibited obvious short-term memory improvement activity on an Alzheimer's disease fly model.

© 2021 Chinese Pharmaceutical Association and Institute of Materia Medica, Chinese Academy of Medical Sciences. Production and hosting by Elsevier B.V. This is an open access article under the CC BY-NC-ND license (<http://creativecommons.org/licenses/by-nc-nd/4.0/>).

1. Introduction

A large number of facts have shown that fungus is one of major sources for searching novel molecules¹. *Sporormiella* is a genus of Ascomycete fungi in the family Sporormiaceae, which contains more than 80 species^{2–5} widely distributing in sub-boreal and temperate regions of the world. It is composed of coprophilous species found on the dung of livestock and wild herbivores, and endophytic species living in plants^{6–8}. The spores of these species have dark brown and septate characteristic features, and have a pronounced sigmoid germination pore^{6,7}. These fungi produce a variety of secondary metabolites, including xanthenes, chromones, macrocyclic lactone, organic acids, triterpenoids, steroids, and the nitrogenous compounds^{9,10}.

In our searching for complex and bioactive molecules from fungi^{11–13}, five new tricyclic C–C coupled orsellinic acid derivative dimers with dimethyl cyclopentanone unit (sporormielones A–E) were isolated from a strain of fungus *Sporormiella* sp. 40-1-4-1, which were derived from a polyketide precursor (3-methylcorticaldehyde) produced by the NR-PKS gene (*spoA*)¹⁴. In order to find more novel compounds, a further chemical investigation on this strain was carried out, which led to the isolation of three complex polyketides (tripodalsporormielones A–C, **1–3**) possessing unprecedented cage-like skeletons with polydent bridged and fused ring systems (Fig. 1). Herein, we described the structural elucidations and bioassays of tripodalsporormielones A–C (**1–3**). Furthermore, the plausible biosynthetic pathway of **1–3** was proposed.

2. Results

The EtOAc extract of *Sporormiella* sp. 40-1-4-1 fermented with rice was subjected to silica gel column chromatography using cyclohexane/MeOH (100:0 and 0:100, v/v) to afford a cyclohexane extract and a MeOH extract. The MeOH extract was subjected to ODS and preparative HPLC to afford three novel polyketides (tripodalsporormielones A–C, **1–3**). Their structures, including absolute configurations, were determined by NMR, X-ray, calculated NMR and ECD experiments.

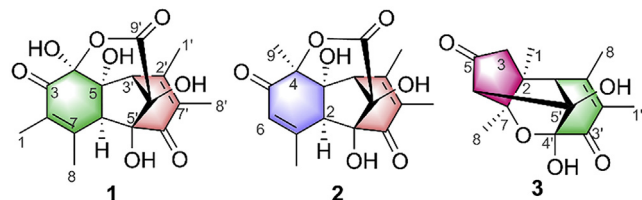


Figure 1 Structures of tripodalsporormielones A–C (**1–3**).

2.1. Structural elucidation of three novel polyketides

Tripodalsporormielone A (**1**) was isolated as yellow crystals, and its molecular formula was deduced as C₁₇H₁₈O₈ based on a pseudomolecular ion peak at *m/z* 351.1076 [M + H]⁺ (Calcd. for C₁₇H₁₉O₈, 351.1080) by HRESIMS, indicating nine degrees of unsaturation. The ¹H NMR spectrum (Supporting Information Table S1) showed two methine protons (δ_{H} 3.30 and 2.77) and four methyls (δ_{H} 2.02, 1.82, 1.80, and 1.75). The ¹³C NMR spectrum only showed 16 carbon signals, which indicated one unobserved carbon existing in ¹³C NMR experiment compared with HRESIMS. Combined with DEPT 135 spectrum, these observed ¹³C resonances can be ascribable to two ketone carbonyl carbons (δ_{C} 198.9 and 187.7), one ester carbonyl carbon (δ_{C} 168.8), four aromatic or olefinic non-protonated carbons, three oxygenated non-protonated *sp*³ carbons (δ_{C} 84.4, 82.7, and 75.7), two *sp*³ methine carbons, and four methyl carbons. In the HMBC spectrum, the observed correlations from H₃-1' (δ_{H} 2.02, brs) to C-2' (δ_{C} 151.2)/C-3' (δ_{C} 53.1)/C-7' (δ_{C} 127.9), from H₃-8 (δ_{H} 1.82, brs) to C-2 (δ_{C} 128.3)/C-6 (δ_{C} 53.0)/C-7 (δ_{C} 150.7), from H₃-8' (δ_{H} 1.80, brs) to C-2' (δ_{C} 151.2)/C-6' (δ_{C} 198.9)/C-7' (δ_{C} 127.9), and from H₃-1 (δ_{H} 1.75, brs) to C-2 (δ_{C} 128.3)/C-3 (δ_{C} 187.7)/C-7 (δ_{C} 150.7) revealed the existence of two dimethylbut-2-enoyl moieties. In addition, the HMBC correlations from H-3' (δ_{H} 3.30, brs) to C-6 (δ_{C} 53.0)/C-9' (δ_{C} 168.8), from H-6 (δ_{H} 2.77, brs) to C-7 (δ_{C} 150.7)/C-6' (δ_{C} 198.9), and from H-6/H-3' to three oxygenated non-protonated *sp*³ carbons (δ_{C} 84.4, 82.7, and 75.7) were observed. Since the HMBC correlations from H-6/H-3' to these three oxygenated non-protonated *sp*³ carbons were hardly identified as ³J_{CH} or ⁴J_{CH} correlations, three plausible topological structures (Fig. 2) were enumerated based on the observed HMBC

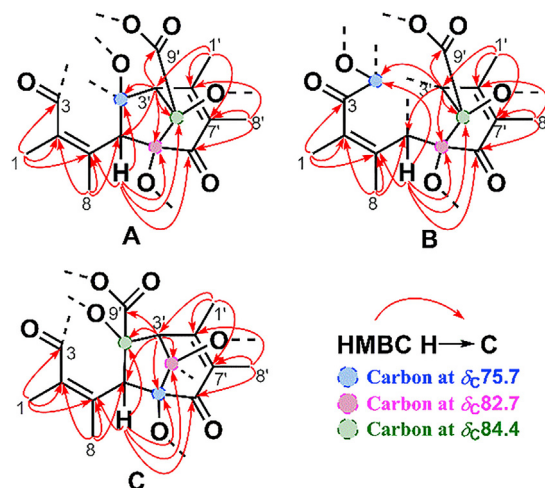


Figure 2 Plausible topological structures of **1**.

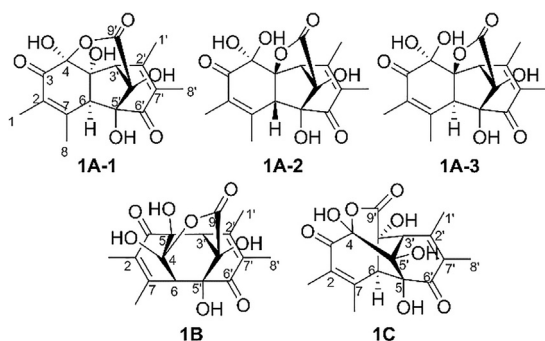


Figure 3 Plausible structure candidates of **1**.

Table 1 Related parameters of the calculated ^{13}C chemical shifts for five structure candidates of **1**.

Parameter	1A-1	1A-2	1A-3	1B	1C
R^2	0.9967	0.9942	0.9951	0.9963	0.9978
MAE	2.42	3.83	3.44	3.07	2.45
MaxErr	11.18	10.79	10.59	8.26	6.40
DP4	70.43%	0.00%	0.00%	0.01%	29.56%

R^2 : correlation coefficient in regression analysis. MAE: mean absolute error. MaxErr: maximum absolute error.

correlations and chemical shifts. What is more, the unobserved carbon in ^{13}C NMR was still undetected in 2D NMR experiments, which made the structural elucidation more complicated. On the basis of the molecular formula, the degrees of unsaturation, the possible linkage of ester bond, and structural rationality (*e.g.*, reasonable chemical shift, bond length, and bond angle), these three plausible topological structures (A–C, Fig. 2) would lead to five plausible structure candidates (Fig. 3). For lacking important HMBC correlations, only using NMR is hard to obtain the accurate structure of **1** with a high non-protonated carbon-containing system from these plausible structure candidates (Fig. 3).

NMR calculation has been commonly used in structural elucidation and revision of natural products¹⁵. Therefore, NMR calculations of these candidates were carried out using GIAO method at the mPW1PW91/6-31+G(d,p) level in the IEFPCM solvent model (DMSO). Based on DP4 evaluation^{16,17}, the structure of **1** was inferred as **1A-1** (Table 1), and the chemical shift of the unobserved carbon (C-4) was predicted as 96.1 ppm according to the NMR calculation. Finally, X-ray data of **1** was obtained and unambiguously showed the whole structure of **1** with its relative configuration as $4S^*$, $5S^*$, $6S^*$, $3'S^*$, $4'S^*$, $5'S^*$ (Fig. 4), which confirmed the deduction from NMR calculation.

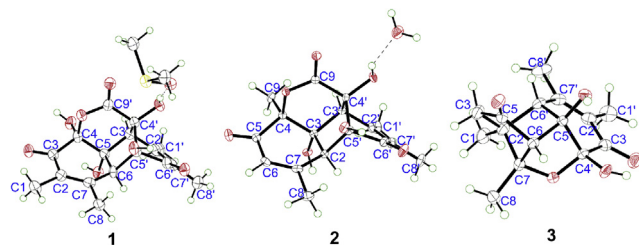


Figure 4 X-ray crystal diffractions of **1–3**.

Tripodalsporormielone B (**2**) was purified as yellow crystals, and its positive HRESIMS gave the molecular formula of $\text{C}_{17}\text{H}_{18}\text{O}_7$ from a pseudomolecular ion peak at m/z 335.1124 [$\text{M} + \text{H}$]⁺ (Calcd. for $\text{C}_{17}\text{H}_{18}\text{O}_7$, 335.1131). The ^1H and ^{13}C NMR data (Supporting Information Table S2) of **2** suggested the presences of four methyl groups (δ_{H} 2.02, 1.91, 1.81, and 1.52; δ_{C} 24.0, 22.4, 15.5, and 10.9) and three carbonyl groups (δ_{C} 198.2, 191.2, and 167.6). The HMBC correlations from $\text{H}_3\text{-1}'$ (δ_{H} 2.02, brs) to C-2'/C-3'/C-7', from $\text{H}_3\text{-8}'$ (δ_{H} 1.81, brs) to C-2'/C-6'/C-7', and from $\text{H}_3\text{-3}'$ (δ_{H} 3.39, s) to C-4'/C-5'/C-9' indicated the presence of dimethylcyclohex-2-enone fragment, which was the same as that of **1**. The other observable HMBC correlations from $\text{H}_3\text{-8}$ (δ_{H} 1.91, brs) to C-2/C-6/C-7, from $\text{H}_3\text{-9}$ (δ_{H} 1.52, s) to C-3/C-4/C-5, from H_2 (δ_{H} 2.88, brs) to C-3/C-7/C-4'/C-5'/C-6', from $\text{H}_3\text{-3}'$ (δ_{H} 3.39, s) to C-2/C-4, and from H_6 (δ_{H} 6.01, brs) to C-4/C-8 expanded the fragment and gave the partial structure of **2** (Fig. 5). Since no further useful NMR information was found, the linkage of ester bond was hard to be determined. Finally, the complete structure of **2** was established by X-ray data (Fig. 4), and its relative configuration was determined as $4S^*$, $5S^*$, $6S^*$, $3'S^*$, $4'S^*$, $5'S^*$. The observed ROESY correlations between $\text{H}_3\text{-3}'$ and $\text{H}_3\text{-9}/\text{H}_3\text{-1}'$ were consistent with the above deduction.

Tripodalsporormielone C (**3**) was obtained as yellow crystals. Its molecular formula was determined as $\text{C}_{15}\text{H}_{18}\text{O}_5$ on the basis of the protonated molecular ion at m/z 279.1228 [$\text{M} + \text{H}$]⁺ (Calcd. for $\text{C}_{15}\text{H}_{19}\text{O}_5$, 279.1232) in its HRESIMS. Two carbonyl carbon signals (δ_{C} 209.3 and 191.1), two olefinic non-protonated carbons (δ_{C} 153.4 and 126.6), four non-protonated sp^3 carbon signals (including three oxidized ones, δ_{C} 96.3, 92.3, and 87.0), two sp^3 methine carbon signals (δ_{C} 67.6 and 56.1), one sp^3 methylene signal (δ_{C} 52.9), and four methyl carbon signals (δ_{C} 23.0, 14.7, 12.1, and 10.7) were found in ^{13}C NMR spectrum (Supporting Information Table S3). The HMBC correlations from $\text{H}_3\text{-8}'$ (δ_{H} 1.96, brs) to C-2'/C-6'/C-7', from $\text{H}_3\text{-1}'$ (δ_{H} 1.73, brs) to C-2'/C-3'/C-7', and from H_6' (δ_{H} 2.39, brs) to C-4'/C-5' indicated the presence of dimethylcyclohex-2-enone moiety in **3**, which was also similar with that of **1**. The other observable HMBC correlations from $\text{H}_3\text{-8}$ (δ_{H} 1.16, s) to C-2/C-6/C-7, from $\text{H}_3\text{-1}$ (δ_{H} 0.98, s) to C-2/C-3/C-7, from $\text{H}_2\text{-3}$ (δ_{H} 2.35) to C-2/C-5/C-6/C-6', and from H_6 (δ_{H} 2.89, s) to C-5/C-4'/C-5'/C-6' indicated the existence of a dimethylbicyclo[2.2.1]heptan-2-one moiety. Based on the molecular formula and the degrees of unsaturation, the partial structure of **3** (Fig. 5) was established. However, the limited NMR data would not establish the complete structure. Finally, X-ray crystal diffraction of **3** (Fig. 4) established the whole planar structure and the relative configuration of **3** as $2S^*$, $6R^*$, $7S^*$, $4'R^*$, $5'R^*$, $6'S^*$. In addition, the observed ROESY correlations between H_6' and H_1/H_8' , between H_8' and H_1 , between H_1 and H_3/H_8 , and between H_6 and H_8 were consistent with the above deduction. Therefore, the structure of tripodalsporormielone C (**3**) was also established, which was a 7-oxatetracyclo[6.3.1.0^{2,6}.0^{5,12}]undecane skeleton as a tripodal bridged and fused ring system (Fig. 1).

The optical rotation data of **1–3** were close to zero and the space groups of X-ray crystal data of **1–3** were achiral ($P\bar{1}$ for **1**, $P2_1/n$ for **2**, $P2_1/n$ for **3**), which indicated that **1–3** should be the mixtures of enantiomers. So, chiral HPLC analyses of **1–3** were carried out. Except for **2**, the enantiomers of **1** and **3** were successfully isolated by the chiral HPLC chromatography with the existing conditions, respectively. Two pairs of enantiomers [(–) **1a**/(+) **1b** and (+) **3a**/(–) **3b**] were obtained (Supporting Information Figs. S1 and S2). After that, the quantum chemical electronic circular dichroism (ECD) calculations of

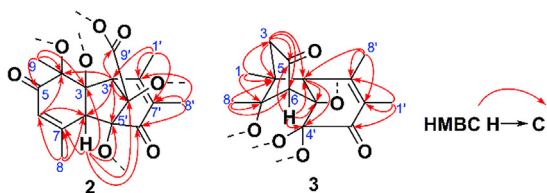


Figure 5 Key HMBC correlations of **2** and **3**.

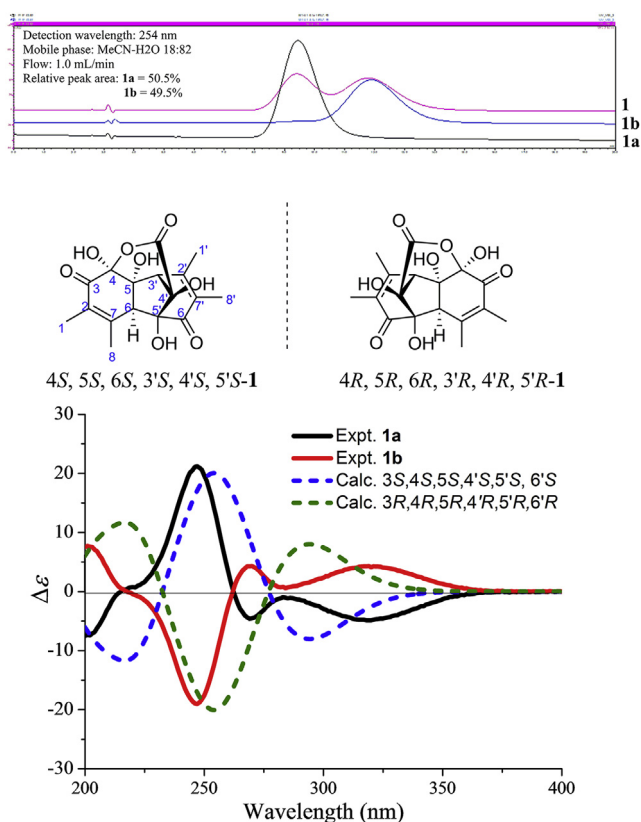


Figure 6 Chiral HPLC analysis, experimental and calculated ECD spectra of **1**.

(4*S*,5*S*,6*S*,3'*S*,4'*S*,5'*S*)-**1** and (4*R*,5*R*,6*R*,3'*R*,4'*R*,5'*R*)-**1** were used to determine their absolute configurations. The calculated ECD data were obtained at the B3LYP/TZVP level in MeOH. The predicted ECD curve of (4*S*,5*S*,6*S*,3'*S*,4'*S*,5'*S*)-**1** matched well with the experimental spectrum of (–) **1a** (Fig. 6), indicating the absolute configuration of (–) **1a** to be 4*S*, 5*S*, 6*S*, 3'*S*, 4'*S*, 5'*S*. As well, the absolute configuration of (+) **1b** was determined as 4*R*, 5*R*, 6*R*, 3'*R*, 4'*R*, 5'*R*. Similarly, the absolute configurations of (+) **3a** and (–) **3b** were determined as 2*S*,6*R*,7*S*,4'*R*,5'*R*,6'*S*-**3** and 2*R*,6*S*,7*R*,4'*S*,5'*S*,6'*R*-**3** based on ECD calculation (Supporting Information Fig. S12) with the same calculated system, respectively.

2.2. Bioactive screenings of novel polyketides

The bioactivities of **1** and **3** were screened on rescuing AD (Alzheimer's disease) flies short-term memory, anti-

acetylcholinesterase (AChE), cytotoxicity, and antimicrobial assays, and **1** showed obviously improving activity to save short-term memory of AD flies with the performance indexes (PI) 43.5 ± 10.6 (Supporting Information Fig. S13), which was similar to the positive control (memantine, PI = 45.0 ± 6.4).

3. Discussion

Inspired by previous work¹⁴, tripodalsporormielones A–C (**1–3**) would be C–C coupled orsellinic acid derivative dimers and are likely to be derived from the same precursor as sporormielones A–E, whose biosynthesis is initiated by a 3-methylorcinolaldehyde synthase SpoA. Different from sporormielones A–E produced by a single *ortho*-quinone methide (*o*-QM) intermediate, **1–3** would be generated from *para*-QM intermediate and *para*-QM-like intermediate, which are highly reactive chemical motifs^{18,19}. The intermediates I and III would be generated from 3-methylorcinolaldehyde *via* oxidation, demethylation, reduction, and dehydration^{14,20}, while the intermediate II would be derived from 3-methyl orsellinic acid *via* decarboxylation and oxidation (Fig. 7). In the proposed biosynthesis of sporormielones A–E¹⁴, the dimerization would be generated from the same *o*-QM intermediate with different C–C coupled patterns *via* Michael addition. Different from sporormielones A–E, **1–3** would be generated through diverse nucleophilic additions. In the biosynthesis of **1–3**, the intermediates Ia and IIIa undergo dimerization to produce intermediate A followed by nucleophilic addition between 9'-COOH and 4-ketone carbonyl to afford **1**. Similarly, dimerization of intermediates II and Ia would generate intermediate B, which would be converted to **2** by esterification between 9'-COOH and 4-OH. The formation of skeleton of **3** is more complicated than those of **1** and **2**. The intermediates IIIa and IIIb would yield intermediate C-1, which would be converted to **3** by the following enol interconversion, acyloin rearrangement^{21–23}, reduction, and demethylation (Fig. 7).

To date, only a few C–C coupled orsellinic acid derivative dimers have been reported from fungi, including dicyclic ring system (such as oosporins^{24–26} and epicoccolide B²⁷), tricyclic fused ring system (such as sporormielones A–E¹⁴), and simple bridged ring system (such as epicoccolide A²⁷ and epicocconigrone A²⁸). Different from all those reported ones, tripodalsporormielones A–C (**1–3**) are a new class of orsellinic acid derivative dimer possessing more complex skeletons with polydent bridged and fused ring systems. Combined with sporormielones, our work shows that 3-methylorcinolaldehyde would be transformed into various QM and QM-like intermediates in this strain, which would lead to the abundant structural diversity of C–C coupled orsellinic acid derivative polymers with complex skeletons. In addition, these complex molecules are characterized as a high non-protonated carbon-containing system, which results in few HMBC correlations observed. What is more, some signals of non-protonated *sp*² carbons are weak and even unobservable. These would increase the difficulty of the structural elucidation. Our work also clearly exhibits that NMR calculation with DP4 evaluation is a powerful and reliable tool in structural elucidation, which would effectively remove the wrong structure candidates.

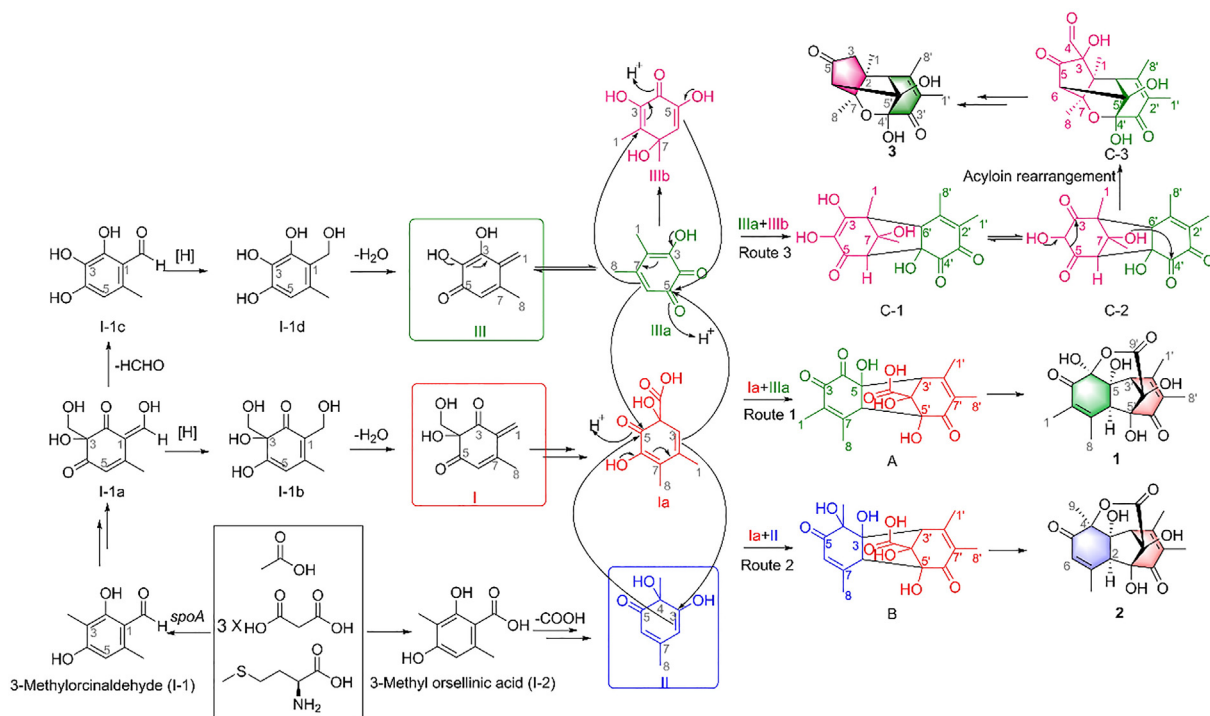


Figure 7 Plausible biosynthetic pathway of tripodalsporormielones A–C (1–3).

4. Experimental

4.1. General experimental procedures

Methanol (MeOH) was purchased from Yuwang Industrial Co., Ltd. (Yucheng, China). Acetonitrile (MeCN) was obtained from Oceanpak Alexative Chemical Co., Ltd. (Gothenburg, Sweden). Ethyl acetate (EtOAc) and cyclohexane were analytical grade from Fine Chemical Co., Ltd. (Tianjin, China).

Melting points were measured on a BÜCHIB-545 melting point measurement (BÜCHI Labortechnik AG, Flawil, Switzerland) without correction. UV data were recorded using a JASCO V-550 UV/Vis spectrometer (Jasco International Co., Ltd., Tokyo, Japan). IR data were recorded on a JASCO FT/IR-480 plus spectrometer (Jasco International Co., Ltd., Tokyo, Japan). Optical rotations were measured on a JASCO P1020 digital polarimeter (Jasco International Co., Ltd., Tokyo, Japan). ECD spectra were recorded in MeOH using a Chirascan-plus qCD spectrometer (Applied Photophysics Ltd., UK) at room temperature. HRESIMS spectra were obtained on Waters Synapt G2 TOF mass spectrometer (Waters Corporation, Milford, USA). 1D and 2D NMR spectra were acquired with Bruker AV 600 spectrometers (Bruker BioSpin Group, Faellanden, Switzerland) using the solvent signals (DMSO- d_6 : δ_H 2.50/ δ_C 39.5) as internal standards. Column chromatography (CC) was carried out on silica gel (200–300 mesh) (Qingdao Haiyang Chemical Group Corporation, Qingdao, China), ODS (50 μ m, YMC), and Sephadex LH-20 (Amersham Pharmacia Biotech, Sweden). TLC was performed on precoated silica gel plate (SGF254, 0.2 mm, Yantai Chemical Industry Research Institute, China). Analytical HPLC was performed on a Dionex HPLC system equipped with an Ultimate 3000 pump, an Ultimate 3000 diode array detector, an Ultimate 3000 column compartment, an Ultimate 3000 autosampler (Dionex, USA), and an Alltech (Grace) 2000 ES evaporative light scattering detector

(Alltech, USA) using a Phenomenex Gemini C18 column (4.6 mm \times 250 mm, 5 μ m). Semi-preparative HPLC and preparative HPLC were carried out on a Shimadzu LC-6AD system equipped with a UV detector. Medium pressure liquid chromatography (MPLC) was performed on ODS (50 μ m) and equipped with a dual pump gradient system, a UV preparative detector, and a Dr Flash II fraction collector system (Shanghai Lisui E-Tech Co., Ltd., Shanghai, China).

4.2. Fungal materials and fermentation

The strain (40-1-4-1) was isolated from the lichen *Cladonia subulata* (L.) Wigg. collected from Changbai Mountain, Jilin province, in August 2006. The strain was identified as *Sporormiella* sp. by Prof. Liangdong Guo and Prof. Dan Hu based on its morphological characteristics and gene sequence analysis. The ribosomal internal transcribed spacer (ITS) and the 5.8S rRNA gene sequences (ITS1-5.8S-ITS2) of the strain have been deposited at GenBank as MK942641.

The fungal strain was cultured on slants of potato dextrose agar (PDA) at 25 °C for 3 days. Agar plugs were used to inoculate 25 Erlenmeyer flasks (500 mL), each containing 100 mL of potato dextrose broth (PDB). Fermentation was carried out in 200 Erlenmeyer flasks (500 mL), each containing 70 g of rice. Distilled H₂O (105 mL) was added to each flask, and the rice was soaked overnight before autoclaving at 120 °C for 30 min. After cooling down to the room temperature, each flask was inoculated with 10.0 mL of the seed culture containing mycelia and incubated at 27 °C for 50 days.

4.3. Extraction and isolation

The culture was extracted thrice with EtOAc, and the pooled organic solvent was evaporated to dryness under vacuum to afford

a crude extract (115.1 g). Then the crude extract was subjected to silica gel CC (4 × 15 cm) using cyclohexane-MeOH (100:0 and 0:100, *v/v*) to afford a cyclohexane extract (C, 70.4 g) and a MeOH extract (w, 38.5 g). The MeOH extract (w, 38.5 g) was separated by ODS MPLC (4 × 30 cm) eluting with MeOH–H₂O (30:70, 50:50, 70:30, 100:0, MeOH–CHCl₃ 1:1 *v/v*) to afford 5 fractions (w1–w5). Fraction w1 (19.7 g) was further subjected to ODS MPLC (4 × 45 cm) eluted with a gradient of MeOH/H₂O (5:95 to 100:0, *v/v*) for 800 min at a flow rate of 20 mL/min to afford fractions w1-1 to w1-6. Fraction w1-4 (9.0 g) was subjected to preparative HPLC on Marchal C18 6 μ C18 column (6 μm, 50 mm × 250 mm) using MeOH/H₂O (18:82, *v/v*) at a flow rate of 100 mL/min with a Newstyle-NP7000 preparative HPLC to afford 3 fractions (w1-4-1–w1-4-3). Fraction w1-4-1 (1.4 g) was subjected to semi-preparative HPLC using MeCN/H₂O (8:92, *v/v*) at a flow rate of 3 mL/min to afford 8 fractions (w1-4-1-1–w1-4-1-8). Fraction w1-4-1-5 (96.9 mg) was subjected to preparative HPLC on Phenomenex Kinetex C8 column (5 μm, 21.2 mm × 250 mm) using MeCN/H₂O (5:95, *v/v*) at a flow rate of 8 mL/min to afford **1** (*t_R*: 33 min, 15.0 mg). Fraction w1-4-1-4 (64.3 mg) was subjected to semi-preparative HPLC on YMC-Pack ODS-A column (5 μm, 10.0 mm × 250 mm) using MeOH/H₂O (10:90, *v/v*) at a flow rate of 3 mL/min to afford **2** (*t_R*: 30 min, 2.0 mg). Fractions w1-4-2 (775.3 mg) and w1-4-3 (264.6 mg) combined with fraction w1-5 (1.53 g) were subjected to Sephadex LH-20 using MeOH to afford 7 fractions (w1-5-1–w1-5-7). Fraction w1-5-4 (983.9 mg) was subjected to semi-preparative HPLC on YMC-Pack ODS-A column (5 μm, 10.0 mm × 250 mm) using MeCN/H₂O (12:88, *v/v*) at a flow rate of 3 mL/min to afford 9 fractions (w1-5-4-1–w1-5-4-9). Fraction w1-5-4-6 (90.2 mg) was subjected to semi-preparative HPLC on YMC-Pack ODS-A column (5 μm, 10.0 mm × 250 mm) using MeCN/H₂O (20:80, *v/v*) at a flow rate of 3 mL/min to afford **3** (*t_R*: 50 min, 13.4 mg).

4.4. Chiral separations of **1** and **3**

The chiral HPLC separation of compound **1** was separated successfully to obtain **1a** [*t_R*: 8.0 min [$[\alpha]_D^{29} = -24.1$ (*c* 1.0, MeOH)]/**1b** [*t_R*: 11.0 min [$[\alpha]_D^{29} = +21.8$ (*c* 1.0, MeOH)] by using an EnantioPak OZ-3 (5 μm, 4.6 mm × 250 mm) at the rate of 1.0 mL/min.

The chiral HPLC separation of compound **3** was separated successfully to obtain **3a** [*t_R*: 17.0 min [$[\alpha]_D^{33} = +192.8$ (*c* 0.129, MeOH)]/**3b** [*t_R*: 20.0 min [$[\alpha]_D^{33} = -189.8$ (*c* 0.091, MeOH)] by using an EnantioPak OZ-3 (5 μm, 4.6 mm × 250 mm) at the rate of 1.0 mL/min.

4.5. Structural characterizations of **1**–**3**

Compound **1**: yellow crystals (MeOH); m.p. 194–199 °C; ESI-MS (positive): *m/z* 351 [M + H]⁺, *m/z* 723 [2M + Na]⁺; HRESIMS (positive) *m/z* 351.1076 [M + H]⁺ (Calcd. for C₁₇H₁₉O₈, 351.1080); UV (MeOH) λ_{max} (log ε) 250 (4.02) nm; IR (KBr) ν_{max} 3470, 2925, 1755, 1671, 1624, 1378, 1338, 1205, 1173, 1034 cm⁻¹; ¹H and ¹³C NMR see Table S1.

(–) (4*S*,5*S*,6*S*,3′*S*,4′*S*,5′*S*) **1a**: [$[\alpha]_D^{29} = -24.1$ (*c* 1.0, MeOH)]; ECD (2.8 × 10⁻⁴ mol/L, MeOH) λ_{max} (Δε): 202 (–7.27), 247 (+21.22), 269 (–4.68), 320 (–5.11) nm.

(+) (4*R*,5*R*,6*R*,3′*R*,4′*R*,5′*R*) **1b**: [$[\alpha]_D^{29} = +21.8$ (*c* 1.0, MeOH)]; ECD (3.2 × 10⁻⁴ mol/L, MeOH) λ_{max} (Δε): 202 (+7.71), 247 (–19.00), 269 (+4.10), 319 (+4.25) nm.

Compound **2**: yellow crystals (MeOH); m.p. 197–203 °C; ESI-MS (positive): *m/z* 335 [M + H]⁺, *m/z* 357 [M + Na]⁺; HRESIMS (positive) *m/z* 335.1124 [M + H]⁺ (Calcd. for C₁₇H₁₉O₇, 335.1131); UV (MeOH) λ_{max} (log ε) 205 (4.00), 230 (4.08) nm; IR (KBr) ν_{max} 3418, 2921, 2900, 1758, 1677, 1626, 1380, 1211, 1170, 1037, 804 cm⁻¹. ¹H and ¹³C NMR see Table S2.

Compound **3**: yellow crystals (MeOH); m.p. 189–194 °C; ESI-MS (positive): *m/z* 279 [M + H]⁺, *m/z* 579 [2M + Na]⁺; HRESIMS (positive) *m/z* 279.1228 [M + H]⁺ (Calcd. for C₁₅H₁₉O₅, 279.1232); UV (MeOH) λ_{max} (log ε) 216 (3.82), 259 (3.80) nm; IR (KBr) ν_{max} 3383, 2986, 2960, 1761, 1673, 1595, 1387, 1355, 1132, 953 cm⁻¹; ¹H and ¹³C NMR see Table S3.

(+) (2*S*,6*R*,7*S*,4′*R*,5′*R*,6′*S*) **3a**: [$[\alpha]_D^{33} = +192.8$ (*c* 0.129, MeOH)]; ECD (2.6 × 10⁻⁴ mol/L, MeOH) λ_{max} (Δε): 202 (+15.38), 236 (+7.66), 268 (–15.05), 328 (+6.63) nm.

(–) (2*R*,6*S*,7*R*,4′*S*,5′*S*,6′*R*) **3b**: [$[\alpha]_D^{33} = -189.8$ (*c* 0.091, MeOH)]; ECD (1.5 × 10⁻⁴ mol/L, MeOH) λ_{max} (Δε): 202 (–15.79), 237 (–8.07), 268 (+17.23), 329 (–7.81) nm.

Acknowledgments

This work was financially supported by grants from National Key Research and Development Program of China (2018YFA0903200/2018YFA0903201), the National Natural Science Foundation of China (81925037 and 81973213), Chang Jiang Scholars Program (Young Scholar) from the Ministry of Education of China (Hao Gao, 2017), National High-level Personnel of Special Support Program (2017RA2259, China), the 111 Project of Ministry of Education of the People's Republic of China (B13038), the Guangdong Natural Science Funds for Distinguished Young Scholar (2017A03036027, China), Local Innovative and Research Teams Project of Guangdong Pearl River Talents Program (2017BT01Y036, China), and K. C. Wong Education Foundation (Hao Gao, 2016, China). The short-term memory assay was supported by Suzhou Joekai Biotechnology LLC. The calculations were supported by the high-performance computing platform of Jinan University.

Author contributions

This work was designed and supported by Prof. Hao Gao, Prof. Xinsheng Yao, and Prof. Dan Hu. The isolations, structural elucidations, calculated ECD and NMR, and the fungal fermentation were performed by Dr. Guodong Chen, Dr. Bingxin Zhao, Miss Meijuan Huang, and Miss Jia Tang. The anti-acetylcholinesterase (AChE), cytotoxicity, and antimicrobial assays were performed by Miss Yanbing Li and Prof. Rongrong He. The fungal strain was supplied by Prof. Liangdong Guo and identified by Prof. Liangdong Guo and Prof. Dan Hu. The paper was written by Dr. Guodong Chen.

Conflicts of interest

The authors declare that they have no competing interests.

Appendix A. Supporting information

Supporting information to this article can be found online at <https://doi.org/10.1016/j.apsb.2021.05.001>.

References

1. Chen GD, Hu D, Gao H, Yao XS. The importance of researches on the fungal bioactive secondary metabolites in developing the comprehensive health industry. *Chin J Nat Med* 2020;**18**:241–2.
2. Ahmed SI, Cain RF. Revision of the genera *Sporormia* and *Sporormiella*. *Can J Bot* 1972;**50**:419–77.
3. Krays A, Eriksson OE, Wedin M. Phylogenetic relationships of coprophilous *Pleosporales* (*Dothideomycetes*, *Ascomycota*), and the classification of some bitunicate taxa of unknown position. *Mycol Res* 2006;**110**:527–36.
4. Wang HK, Aptroot A, Crous PW, Hyde KD, Jeewon R. The phylogenetic nature of *Pleosporales*: an example from *Massariosphaeria* based on rDNA and RBP2 gene phylogenies. *Mycol Res* 2007;**111**:1268–76.
5. Krays A, Wedin M. Phylogenetic relationships and an assessment of traditionally used taxonomic characters in the *Sporormiaceae* (*Pleosporales*, *Dothideomycetes*, *Ascomycota*) utilising multi-gene phylogenies. *Syst Biodivers* 2009;**7**:465–78.
6. Davis OK, Shafer DS. *Sporormiella* fungal spores, a palynological means of detecting herbivore density. *Palaeogeogr Palaeoclimatol Palaeoecol* 2006;**237**:40–50.
7. Mungai PG, Njogu JG, Chukeaitiro E, Hyde KD. Coprophilous ascomycetes in Kenya: *Sporormiella* from wildlife dung. *Mycology* 2012;**3**:234–51.
8. Guo LD, Huang GR, Wang Y. Seasonal and tissue age influences on endophytic fungi of *Pinus tabulaeformis* (Pinaceae) in the Dongling Mountains, Beijing. *J Integr Plant Biol* 2008;**50**:997–1003.
9. Yang BJ, Chen GD, Li YJ, Hu D, Guo LD, Xiong P, et al. A new xanthone glycoside from the endolichenic fungus *Sporormiella irregularis*. *Molecules* 2016;**21**:764.
10. Huang MJ, Li YJ, Tang J, Chen GD, Hu D, Xu W, et al. Spororrminone A and 2-*epi*-spororrminone A, two new chromones from an endolichenic fungus *Sporormiella irregularis*. *Nat Prod Res* 2020;**34**:3117–24.
11. Zhao H, Wang MZ, Chen GD, Hu D, Li EQ, Qu YB, et al. Dimericbiscognienynes B and C: new diisoprenyl-cyclohexene-type meroterpenoid dimers from *Biscogniauxia* sp. *Chin Chem Lett* 2019;**30**:51–4.
12. Zhao H, Chen GD, Zou J, He RR, Qin SY, Hu D, et al. Dimericbiscognienyne A: a meroterpenoid dimer from *Biscogniauxia* sp. with new skeleton and its activity. *Org Lett* 2017;**19**:38–41.
13. Wang CX, Chen GD, Feng CC, He RR, Qin SY, Hu D, et al. Same data, different structures: diastereoisomers with substantially identical NMR data from nature. *Chem Commun* 2016;**52**:1250–3.
14. Chen GD, Hu D, Huang MJ, Tang J, Wang XX, Zou J, et al. Sporormielones A–E, bioactive novel C–C coupled orsellinic acid derivative dimers, and their biosynthetic origin. *Chem Commun* 2020;**56**:4607–10.
15. Willoughby PH, Jansma MJ, Hoye TR. A guide to small-molecule structure assignment through computation of (¹H and ¹³C) NMR chemical shifts. *Nat Protoc* 2014;**9**:643–60.
16. Grimblat N, Zanardi MM, Sarotti AM. Beyond DP4: an improved probability for the stereochemical assignment of isomeric compounds using quantum chemical calculations of NMR shifts. *J Org Chem* 2015;**80**:12526–34.
17. Gao JB, Zhang XJ, Shang K, Zhong WM, Zhang RH, Dai XC, et al. New *seco*-dibenzocyclooctadiene lignans with nitric oxide production inhibitory activity from the roots of *Kadsura longipedunculata*. *Chin Chem Lett* 2020;**31**:427–30.
18. Huang CS, Yang CF, Zhang WJ, De Chandra B, Zhu YG, Jiang XD, et al. Molecular basis of dimer formation during the biosynthesis of benzofluorene-containing atypical angucyclines. *Nat Commun* 2018;**9**:2088.
19. Chu WD, Zhang LF, Bao X, Zhao XH, Zeng C, Du JY, et al. Asymmetric catalytic 1,6-conjugate addition/aromatization of *para*-quinone methides: enantioselective introduction of functionalized diarylmethine stereogenic centers. *Angew Chem Int Ed* 2013;**52**:9229–33.
20. Davison J, al Fahad A, Cai MH, Song ZS, Yehia SY, Lazarus CM, et al. Genetic, molecular, and biochemical basis of fungal tropolone biosynthesis. *Proc Natl Acad Sci U S A* 2012;**109**:7642–7.
21. Hine J, Haworth HW. The mechanism of the benzylic acid rearrangement. *J Am Chem Soc* 1958;**80**:2274–5.
22. Majerski Z, Šarac-Arneri R, Škare D, Lončar B. A facile route to 2-noradamantanone via 4-protoadamantanone. *Synthesis* 1980;**1**:74–5.
23. Xu JF, Zhao HJ, Wang XB, Li ZR, Luo J, Yang MH, et al. (±)-Melicolones A and B, rearranged prenylated acetophenone stereoisomers with an unusual 9-oxatricyclo[3.2.1.1^{3,8}]nonane core from the leaves of *Melicope ptelefolia*. *Org Lett* 2015;**17**:146–9.
24. Love B, Bonner-Stewart J, Forrest L. An efficient synthesis of oosporein. *Tetrahedron Lett* 2009;**50**:5050–2.
25. Ramesha A, Venkataramana M, Nirmaladevi D, Gupta V, Chandranayaka S, Srinivas C. Cytotoxic effects of oosporein isolated from endophytic fungus *Cochliobolus kusanoi*. *Front Microbiol* 2015;**6**:870.
26. Feng P, Shang YF, Cen K, Wang CS. Fungal biosynthesis of the bibenzoquinone oosporein to evade insect immunity. *Proc Natl Acad Sci U S A* 2015;**112**:11365–70.
27. Talontsi F, Dittrich B, Schöffler A, Sun H, Laatsch H. Epicoccolides: antimicrobial and antifungal polyketides from an endophytic fungus *Epicoccum* sp. associated with *Theobroma cacao*. *Eur J Org Chem* 2013;**2013**:3174–80.
28. El Amrani M, Lai DW, Debbab A, Aly AH, Siems K, Seidel C, et al. Protein kinase and HDAC inhibitors from the endophytic fungus *Epicoccum nigrum*. *J Nat Prod* 2014;**77**:49–56.